electronics

Article

Unit Sizing and Feasibility Analysis of Green Hydrogen Storage Utilizing Excess Energy for Energy Islands

Kemal Koca [1], Erkan Dursun [2], Eyüp Bekçi [3], Suat Uçar [4], Alper Nabi Akpolat [2,*], Maria Tsami [5], Teresa Simoes [6,*], Luana Tesch [7], Ahmet Aksöz [8] and Ruben Paul Borg [9]

1 Department of Mechanical Engineering, Abdullah Gül University, 38080 Kayseri, Türkiye; kemal.koca@agu.edu.tr
2 Department of Electrical-Electronics Engineering, Marmara University, 34854 Istanbul, Türkiye; erkandursun@marmara.edu.tr
3 Department of Mechanical Engineering, Harbin Institute of Technology, Shenzhen 518000, China; 25sf53023@stu.hit.edu.cn
4 Tigris Development Agency, 47200 Mardin, Türkiye; suat.ucar@dika.org.tr
5 Department of Economics, School of Economics and Regional Studies, University of Macedonia, 156 Egnatia Street, GR-54636 Thessaloniki, Greece; tsami@uom.edu.gr
6 National Laboratory of Energy and Geology—LNEG, 1649-038 Lisbon, Portugal
7 Department of Civil Engineering, ISISE, ARISE, University of Coimbra, 3030-788 Coimbra, Portugal; luana.tesch@dec.uc.pt
8 Department of Electrical-Electronics Engineering, Kayseri University, 38380 Kayseri, Türkiye; ahmetaksoz@kayseri.edu.tr
9 Faculty for the Built Environment, University of Malta, MSD 2080 Msida, Malta; ruben.p.borg@um.edu.mt
* Correspondence: alper.nabi@marmara.edu.tr (A.N.A.); teresa.simoes@lneg.pt (T.S.)

Abstract

This study examines whether green hydrogen production using combined wind and solar energy on Marmara Island can meet the island's electricity demand and fuel the fuel needs of a hydrogen-powered ferry. A hybrid system consisting of a 10 MW wind farm, a 3 MW solar PV system, and a PEM electrolyzer sized to meet the island's hydrogen demand was modeled for the island, located in the southwestern Sea of Marmara. The hydrogen production potential, energy flows, and techno-economic performance were evaluated using HOMER-Pro 3.18.4 version. According to the simulation results, the hybrid system generates approximately 62.6 GWh of electricity annually, achieving an 82.8% renewable energy share. A significant portion of the produced energy is transferred to the electrolyzer, producing approximately 729 tons of green hydrogen annually. The economic analysis demonstrates that the system is financially viable, with a net present cost of USD 61.53 million and a levelized energy cost of USD 0.175/kWh. Additionally, the design has the potential to reduce approximately 2637 tons of CO_2 emissions over a 25-year period. The results demonstrate that integrating renewable energy sources with hydrogen production can provide a cost-effective and low-carbon solution for isolated communities such as islands, strengthening energy independence and supporting sustainable transportation options. It has been demonstrated that hydrogen produced by PEM electrolyzers powered by excess energy from the hybrid system could provide a reliable fuel source for hydrogen-fueled ferries operating between Marmara Island and the mainland. Overall, the findings indicate that pairing renewable energy generation with hydrogen production offers a realistic pathway for islands seeking cleaner transportation options and greater energy independence.

Academic Editor: Gianpaolo Vitale

Received: 27 September 2025
Revised: 14 December 2025
Accepted: 16 December 2025
Published: 14 January 2026

Keywords: Marmara Island; green hydrogen; electrolysis; hydrogen storage; unit sizing; energy saving; energy island; levelized cost of energy; excess energy utilization; techno-economic analysis; HOMER-Pro

1. Introduction

Europe is seeing a tremendous development in offshore wind energy and plans to construct substantial capacities in the available waters are moving forward quickly. Anticipated technological cost savings present a significant opportunity to assist Europe's decarbonization efforts. Large-scale offshore wind energy has been announced as a solution to bridge the power supply gap left by the closure of nuclear and fossil fuel plants, together with photovoltaic (PV) output [1]. Countries around the world are increasingly adopting ambitious targets, including binding net-zero targets by 2050, in a concerted effort to limit global temperature increase to 1.5 °C. Essential to achieving this goal is the need to reduce emissions from all energy end-uses. However, prevailing estimates from the International Renewable Energy Agency suggest that even with concerted efforts in energy efficiency, electrification, and renewable energy, only 70% of the required emissions reductions can be achieved through these measures alone. In the face of this shortfall, attention is turning to hydrogen as a key solution, particularly in sectors characterized by higher costs, such as heavy industry, long-distance transport, and seasonal energy storage. Furthermore, the intermittent nature of wind and solar energy has necessitated the exploration of alternative energy production and storage solutions. The electrolysis of water to produce green hydrogen serves as a method for obtaining hydrogen energy while also playing a role in mitigating the intermittency and variability associated with renewable energy sources [2].

Projections show that the integration of hydrogen into the energy mix could potentially contribute a significant 12% of the final energy demand required to meet the 1.5 °C scenario. The versatility of hydrogen as an energy carrier underlines its attractiveness, as it can be produced from a wide range of raw materials and can be used in a wide range of applications [3]. Batteries emerge as formidable contenders in the realm of short-term energy storage, boasting rapid response times of less than 1 s and impressive efficiencies exceeding 90%. These attributes render batteries indispensable for addressing immediate fluctuations in energy supply and demand, providing a reliable means of stabilizing grid operations. However, notwithstanding their commendable performance in short-term applications, batteries confront inherent limitations that impede their efficacy in long-term energy storage scenarios. Notably, the propensity for self-discharge rates exceeding 1% and capacity losses nearing 20% over time present formidable hurdles, hampering their suitability for extended storage durations. In contrast, hydrogen emerges as a compelling alternative poised to address the challenges of large-scale, long-term energy storage [4]. The inherent characteristics of hydrogen, including its remarkable energy density, steadfast stability, and minimal losses, position it as an ideal candidate for meeting the exigencies of sustained energy storage needs. Leveraging hydrogen as an energy carrier holds promise not only in mitigating the limitations associated with battery technologies but also in ushering in a paradigm shift towards scalable and resilient energy storage solutions. Through further exploration and innovation in hydrogen storage and utilization technologies, the potential for realizing a sustainable energy future anchored on the virtues of hydrogen storage beckons, offering a pathway towards enhanced energy security and decarbonization objectives on a global scale.

Despite all of these benefits, it is crucial to remember that hydrogen-based systems have limitations of their own, like performance degradation over time. Catalyst loss and membrane degradation are two examples of factors that can lower system efficiency and raise lifecycle costs [5]. Furthermore, activation, ohmic, and concentration-induced polarization losses that occur over time in PEM-based systems are also significant mechanisms that reduce efficiency during operation [6]. As illustrated in Figure 1, renewable energy sources, such as wind and solar energies, exhibit varying potentials influenced by geographical and meteorological conditions, constituting over 12% of global electricity production in 2022 [7]. Forecasts project this share to surpass one-third of the world's electricity by 2030. Despite their promising trajectory, the intermittent nature of most wind- and solar-based renewables presents challenges in meeting the dynamic load demands across diverse locations, underscoring the need for robust energy storage solutions. Addressing intermittency, especially in resources like solar and wind energies, necessitates the development of efficient systems capable of converting and storing surplus electrical energy. Hydrogen emerges as a compelling alternative energy carrier, poised to play a pivotal role in future energy landscapes due to its storability, transportability, and high calorific value. In this context, harnessing excess electrical energy through hydrogen production presents a viable pathway, particularly for decentralized electricity supply systems like energy islands. Hybrid wind and solar power systems integrated into self-contained energy islands offer promise by incorporating both short-term and long-term energy storage solutions. While battery energy storage systems (BESSs) serve short-term storage needs admirably with their high charge–discharge efficiency, their limitations in long-term storage due to low energy density, self-discharge, and leakage necessitate complementary solutions. The synergy between BESSs and hydrogen storage holds the potential to significantly enhance the performance and reliability of wind–solar hybrid systems. Electrolysis emerges as a key method for hydrogen production, leveraging renewable energy sources in an environmentally friendly manner, thereby aligning with the goals of environmental sustainability and growth. However, challenges persist in managing interruptions in renewable energy systems and fluctuating power demands, underscored by factors such as system locations and geographical and meteorological variables. The successful mitigation of these challenges hinges on appropriately sizing system components and conducting comprehensive feasibility studies. Thus, this study aims to delve into the sizing and hydrogen production potential of hybrid power systems, integrating wind turbines and photovoltaic modules, with a primary focus on electrolysis-based hydrogen production utilizing renewable energy sources. Through this research endeavor, we aim to contribute to the advancement of sustainable energy solutions and inform decision-making processes in transitioning towards a greener and more resilient energy future.

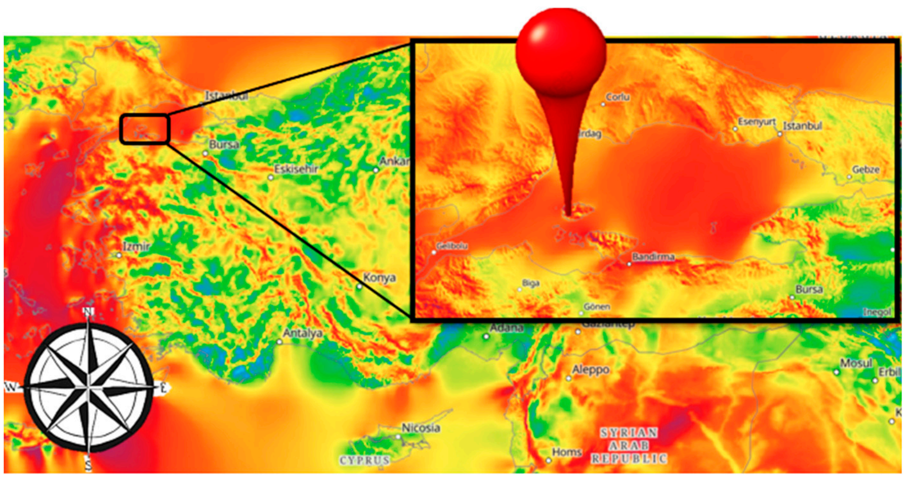

Figure 1. Demonstration region. While hot colors denote more wind potential areas, cold colors do less.

Energy islands, which are a European-born idea, are at the heart of energy transition efforts. Power to X is the process of converting renewable electricity into hydrogen-based energy carriers such as natural gas, liquid fuels, and chemicals. Power to Hydrogen-H_2 is a subset of Power to X, where hydrogen is the green energy obtained from the conversion process [8]. On the other hand, the high dependency of renewable energy systems on geographical and meteorological conditions creates regulatory and control challenges for power system operators. A hybrid system of wind, solar, hydrogen, and energy storage can minimize this problem. As a clean energy carrier, hydrogen can be used in places where population density, geographical constraints, government policies, and regulatory issues preclude the installation of large- or medium-scale renewable energy facilities.

For renewable-based hydrogen production to be utilized on ferries, an appropriate refueling infrastructure is necessary for the island. A shore-based refueling station, where hydrogen produced by electrolyzers is stored at high pressure on land, and ferries refuel through pressure-controlled lines upon berthing, is essential. This method, commonly used in current hydrogen ship projects, offers safe and quick refueling and aligns with the island's renewable energy generation profile. It enables hydrogen made from wind and solar energy to be directly used in ferry operations, lowering transportation emissions and boosting energy independence. This infrastructure could serve as a viable P2H (Power-to-Hydrogen) solution that facilitates the transfer of renewable energy to the transportation sector in isolated systems like islands.

The remainder of this study is structured as follows: Section 2 describes the methodological framework, including the study area, system description, and data analysis. The results and discussion are outlined in Section 3. The conclusion and main findings of the study are summarized in Section 4, and Section 5 explains the limitation and future works of the study.

Overview and Literature Studies

Energy islands are observed to form areas with significant wind power production. The idea of establishing power link islands in a meshing offshore grid is expanded upon in the limited literature now available on this subject [9]. The combination of electricity and hydrogen production from offshore wind farms on massive energy islands was initially analyzed by Singlitico et al. [10]. The authors evaluated various working modes where the priority was either conveyance via electrical infrastructure or conversion to hydrogen, all within a pre-defined setting of electrolyser size and cable connection. They discover that placing facilities offshore can be beneficial and that switching to an operating mode powered by hydrogen can lower the levelized cost of hydrogen to the point where it is competitive with hydrogen derived from fossil fuels. In order to decarbonize the Norwegian continental shelf, Zhang et al. [11] study offshore wind hubs in the North Sea and create a mixed-integer linear investment planning and operations model that minimizes costs. Under particular CO_2 prices, they create scenarios for investments in offshore hubs equipped with hydrogen conversion machinery, storage, transmission of electricity, and renewable energy generation. Additionally, they contend that, in a scenario with moderate CO_2 costs, offshore wind and a cable connection to the shore can cut current emissions in half. Gea Bermúdez et al. [12] revealed in a capacity expansion model (CExM) that onshore hydrogen production is more likely to be cost-efficient due to patterns following PV generation, while driving hydrogen offshore will result in higher system costs. A zonal market representation with cross-border flows serves as the foundation for their research. This method is likely to overestimate the amount of electricity flowing across zones by underestimating inner-zonal congestion. The welfare impacts of a North Sea energy island on the European electrical grid are examined by Tosatto et al. [13]. Their findings, which are consistent with those for offshore grids, indicate that, in an environment where there is no coupling sector and only electricity production, overall welfare will rise, but the distribution of benefits will be asymmetric: consumer welfare will rise while producers' welfare in exporting countries will suffer. Wang et al. [14] developed a wind-based ZCIIES and showed that a zero-carbon island integrated energy system (ZCIIES) is more economical in regions with higher fuel prices and a wealth of renewable energy resources. Based on the Pacific Island nation of Samoa, Vaiaso et al. [15] built a ZCIIES and showed that the profitable operation of ZCIIES could be achieved by a renewable energy system with a specific percentage of energy storage. It is imperative to handle freshwater availability on islands in addition to traditional power, heating, and cooling needs [16]. Although several studies have examined hybrid renewable systems and hydrogen production for islands such as the Azores, Bornholm, and Orkney, these works generally emphasize either grid support or hydrogen export rather than transport-focused hydrogen utilization. The present study differs in three main ways. First, it evaluates an integrated wind–solar–hydrogen system specifically tailored to the energy and transportation needs of Marmara Island, including the hydrogen demand of a real ferry route. Second, the study applies HOMER-Pro software not only for system optimization but also to examine hydrogen production behavior under local seasonal fluctuations, which has not been previously quantified for this region. Third, the work frames Marmara Island as a functional 'energy island' by linking renewable generation, on-site hydrogen conversion, and maritime transport in a unified techno-economic model. Together, these elements extend existing approaches by demonstrating how hybrid systems can be scaled and adapted to support hydrogen-based mobility in isolated communities [17]. Using HOMER-Pro software, this innovative optimization research was carried out for Marmara Energy Island in Turkey, forecasting the need for maritime transportation in the future. The strategic advantage resulting from the island's placement in the convergence of the Istanbul and Çanakkale straits is the primary element that sets this study apart from other research in the literature. This site is intended to serve as a refueling station for long-distance hydrogen-powered ships. The study intends to become a supply and logistics hub for the upcoming hydrogen-powered sea vehicles in addition to meeting the island's own energy demands. The study has a distinctive and innovative character because of its future-oriented and regional needs-focused modeling.

Furthermore, some similar studies have been conducted in the relevant state of the art. For example, by comparing three different 100% renewable-based microgrid scenarios for a university campus (PV–battery–H_2, wind–H_2, and PV–wind–H_2), we identify the lowest-cost system and show that a combination of PV, wind, and green hydrogen is the most economical option. A main goal of this study is to highlight the cost-effectiveness of integrating renewable resources with green hydrogen [18].

A solar- and battery-based microgrid demonstrates significant reductions in energy demand and CO_2 emissions through thermal integration by optimizing hydrogen and dimethyl ether production with an electrolyzer. Regarding this study [19], the technical and economic feasibility of sustainable fuel production is assessed using economic and thermal optimization with the HYSYS V12 software platform and the General Algebraic Modeling System. Techno-economic analyses are generally of great importance. Ref. [20] evaluates the performance of a wind- and biogas-based multi-energy system (electricity, heat, and hydrogen) designed to supply industrial loads and electric vehicle/hydrogen vehicle charging stations. It demonstrates that the off-grid MES structure can significantly reduce multi-generation energy costs by optimizing LCOE, LCOH, and LCOT. Similarly, the authors in [21] analyze large-scale PV–wind–H_2 systems (net metering and islanded mode) with a Python version 3.9.14-based model and find that LCOE and electrolyzer costs are the most influential parameters on LCOH. Their results show that the net metering scenario produces the lowest hydrogen cost and that LCOH can be reduced to USD 1/kg under favorable conditions.

The analyses demonstrate that the 82.8% renewable energy share achieved by the hybrid wind–solar–hydrogen system on Marmara Island is consistent with similar studies in the literature and even outperforms many scenarios. For example, while the renewable energy share in systems integrating PV, wind, and hydrogen in [18,20] generally remains in the 50–80% range, the Marmara Island example approaches the upper limit of this range, demonstrating that high renewable energy penetration at the island scale is technically feasible. Furthermore, the annual hydrogen production of 729 tons and the system's economic viability provide a framework consistent with the LCOH ranges reported in the literature. Refs. [20–22] report hydrogen levelized costs ranging from USD 3 to USD 11/kg. While no direct LCOH value is provided in the Marmara Island scenario, given the energy produced, renewable share, and electrolyzer utilization rate, the system appears to have a cost structure within this range. The study therefore confirms that high renewable penetration can be matched with sustainable hydrogen production and demonstrates, consistent with the literature, that cost-effective, low-carbon energy–fuel integration in island communities is both technically and economically feasible. While many studies [16–22] contribute valuable insights into the technical and economic aspects of renewable energy–hydrogen integration, none focus on a system architecture where island-scale green hydrogen is combined with ferry refueling for maritime transport. Thus, this study offers a unique unit sizing perspective that complements existing models by calculating the annual hydrogen production based on Marmara Island's renewable resources, aligning this production with the yearly fuel requirements of ferry operations and assessing a practical shore-based refueling scenario between the island and the mainland. A simple comparison with most related studies is presented in Table 1.

Table 1. Summary of a comparison table of related methods.

System Configuration	Hydrogen Application	Economic Assumptions/ Limits	Main Difference
PV + wind + H_2 + microgrid [23]	Storage/recycling	General economic model	No ferry application
General H_2 energy strategy [24]	Maritime transport policy	Strategic model	No technical microgrid design
PV + wind + microgrid [25]	No hydrogen	Electrical-based model	No ferry fuel and H_2 demand
Floating PV + H_2 fuel delivery [26]	Ferry	Fuel station economy model	Electrical loads with ferry

2. Materials and Methods

2.1. Demonstration of Pilot Area

The proposed energy island is positioned in the Marmara Sea of Türkiye, as illustrated in Figure 1. Marmara Island, which is located at the west part of the Marmara Sea. Its specific coordinates on the map are 40°39′28.98″ N–27°39′52.69″ E.

Marmara Island is the largest of this group of islands located in the southwest of the Marmara Sea, off the coast of Türkiye, which is accessible by sea from Istanbul, Tekirdağ and Balıkesir (Erdek). The population of the island is about 10,000, but this number can increase up to three times with tourism activity in the summer months. As concerns about sustainability and zero-emission green approaches continue to grow, new and innovative solutions are emerging in transportation. One such solution is the MF Hydra, a state-of-the-art, hydrogen-fueled ferry that promises to revolutionize maritime travel and is already in use in Norway. The MF Hydra can connect Marmara Island and the port town of Erdek, two important points in this part of Türkiye, providing a clean and efficient transportation option for both locals and tourists.

In this section, a technical analysis on the feasibility of the MF Hydra passenger and car ferry running on hydrogen fuel has been carried out. By replacing the ferry currently carrying passengers and cars between Marmara and Erdek with a hydrogen-fueled vessel, it is possible to run this line with zero emissions. This approach not only reduces carbon emissions but also contributes to cleaner air and waterways, benefiting both the environment and public health. Now that there are hydrogen-powered cars and trains across the world, this new project is a sea change for green hydrogen. The ferry running between Marmara Island and Erdek stops at Ekinlik Island, Avşa Island, and Paşalimanı Island, respectively, before reaching its final destination. This route covers 21.08 nautical miles (39 km), as seen in Figure 2.

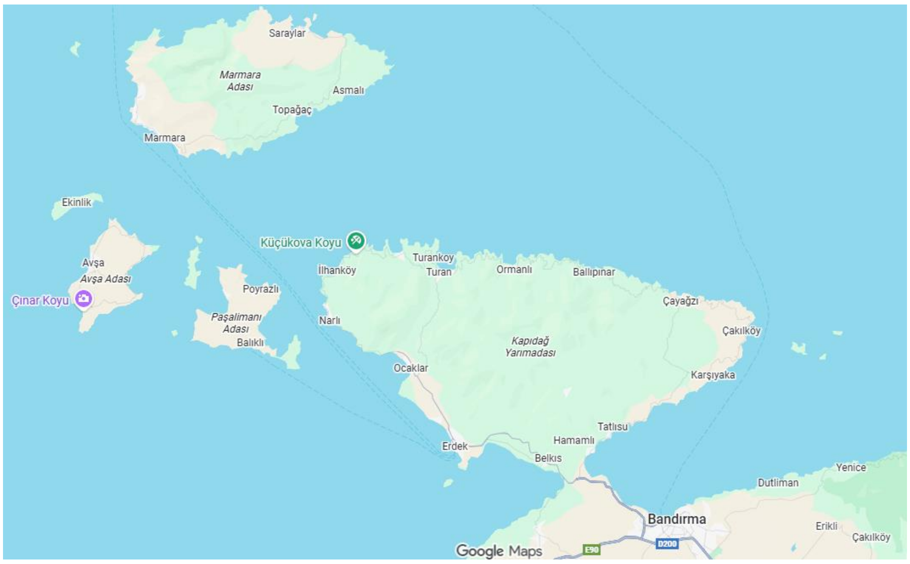

Figure 2. Case study of Marmara Island on the top.

This study calculates the route and fuel consumption based on the MV Sea Change passenger ship as a reference. The MV Sea Change has two engines with a propulsion power of 300 kW each, can store up to 246 kg of hydrogen, and has a speed of 15 knots [27]. This means that it covers the required distance in 1.41 h. The energy requirement for a single trip is 846 kWh, and the daily energy requirement is 1692 kWh. The unit hydrogen consumption is 0.060 kgH_2/kWh. The annual hydrogen demand for 330 days is 34 tons. The 250-bar pressurized hydrogen tanks on the ship are capable of meeting the technical parameters required for the Marmara–Erdek route.

2.2. General System Description

This part of the paper presents a discussion of the HOMER-Pro program, including descriptions and data analysis.

2.2.1. Configuration of HOMER-Pro Software

An analytical program called the hybrid optimization of multiple energy resources (HOMER) optimizer is used worldwide as a standard for the best planning and evaluation of both grid-connected [28,29] and standalone energy systems [30–32]. Numerous energy studies have used HOMER because of its consistency, user-friendly interface, and reliable programming structure. Therefore, HOMER software was utilized to integrate all components and simulate the overall system performance. Key aspects of the integration were included as follows:

- Energy Flow Analysis: The software simulated the energy flow between the wind turbines, PV panels, electrolyzer, batteries, and hydrogen storage. This analysis provided insights into how energy is generated, stored, and utilized within the hybrid system.
- Techno-Economic Evaluation: The simulation included detailed techno-economic analysis, calculating metrics such as Net Present Value (NPV), Levelized Cost of Energy (LCOE), and payback period. These metrics were critical in assessing the financial viability of the hybrid system.
- Environmental Impact Assessment: The potential reduction in CO_2 emissions and other environmental benefits were evaluated, highlighting the system's contribution to sustainability and carbon footprint reduction.

The software's built-in dispatch algorithms control power flow in the HOMER-Pro simulation. Future research could incorporate real-time control mechanisms, like a voltage–power self-regulation framework, for advanced coordination of wind, PV, and electrolyzer units to further improve system resilience under varying renewable energy generation conditions. With the software's optimized logic handling dynamic control, the current study focuses on the long-term techno-economic viability. The utilized parameters in the HOMER-Pro software are given in Table 2.

Table 2. The parameters used in HOMER-Pro.

HOMER-Pro Parameters	
Discount Rate	8%
Inflation Rate	2%
Project Lifetime	25 years
Hub Height of Wind Turbine	80 m
Wind Data	Nasa POWER database (January 1984–December 2013) monthly averages
Solar Data	Nasa POWER database (July 1983–June 2005) monthly averages
Electrolyzer Efficiency	85%
Hydrogen Tank Size	200 kg
Initial Tank Level	50%
Converter Efficiency	95%

The essential target of the system is to produce hydrogen and meet the fuel consumption of the ships by means of desired energy and hydrogen islands. As denoted in Figure 3, the system consisted of a 10 MW wind power plant, the power curve of which is shown in Figure 4, 3 MW PV power plant, and a 13,486 kW electrolyzer for 2000 kg/day hydrogen demand, converter, and grids. PV power plants produce electricity when solar energy is available. Direct load powering is achieved using generated electricity. An electrolyzer uses whatever additional energy is available to create hydrogen. Produced hydrogen is stored in a hydrogen tank and used by a fuel cell to generate power when solar energy is not accessible (because of clouds and dark nights, etc.)

https://doi.org/10.3390/electronics15020362

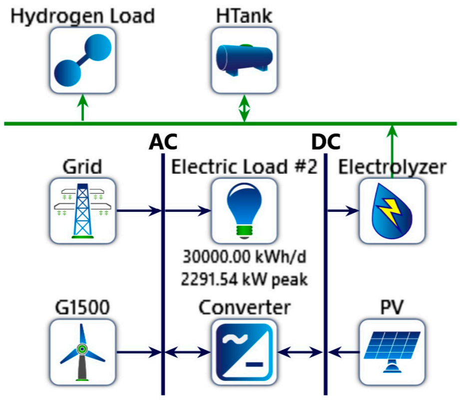

Figure 3. System configuration.

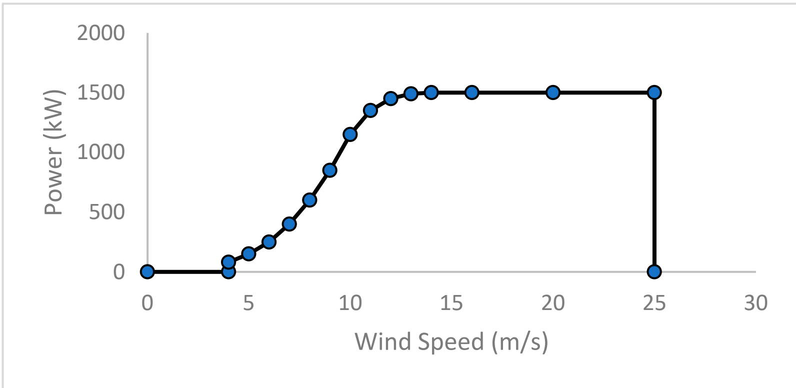

Figure 4. Power curve of a generic 1500 kW wind turbine.

The determination of the hydrogen demand and system sizing in the created energy island model was based on a multi-step optimization process. In the first step, the island's daily energy demand was estimated at 30,000 kWh, based on its current population. In the second step, to meet this demand optimally and utilize surplus energy, various capacities of wind and solar power were introduced as inputs to the model. For instance, solar PV capacities of 2000 kW, 3000 kW, and 5000 kW, along with wind turbine configurations ranging from 1 to 8 units, were analyzed in different hybrid combinations. In the third step, after satisfying the local energy demand, the potential hydrogen production from the resulting surplus energy was estimated. Consequently, different hydrogen load values—such as 1500 kg/day, 2000 kg/day, 2500 kg/day, and 2800 kg/day—were input into the optimization program. An optimization process was then initiated, considering grid power purchase and sales costs as well as the capital and operational costs of the energy systems. The most optimum result was selected from 27,060 feasible solutions and presented in this study.

PEM electrolyser efficiency, modeled as a variable parameter, depends on the load ratio. In HOMER-Pro, PEM efficiency can be adjusted by the user. The figure provides all necessary parameters (hydrogen load, efficiency, energy production, and cost); thus, since degradation is set at 0%, it creates a baseline to the reader for reusability and adaptability. Users may stimulate the program again by using their assumptions related to performance degradation. The efficiency calculation equation is illustrated in Equation (1), which depends on the produced hydrogen mass, the higher heating value, and the consumed electrical energy.

$$\eta_{PEM} = \frac{m_{H2} \cdot HHV_{H_2}}{E_c} \times 100\% \tag{1}$$

where, n_{PEM} is the efficiency of PEM, m_{H2} shows the mass of hydrogen, HHV_{H2} is higher heating value of hydrogen and E_C denotes consumed electrical energy.

To ensure transparency and reproducibility, all major technical and economic parameters used in the simulation were compiled into a dedicated input table (Table 3). These include the capital and replacement costs of PV modules, wind turbines, the PEM electrolyzer, hydrogen storage, converter, and grid electricity tariffs, together with assumed O&M costs, lifetime, degradation considerations, and the discount rate applied in the economic analysis. The parameter values were based on the recent literature and standard cost databases used in HOMER studies. In HOMER-Pro, the hybrid system is optimized primarily through the minimization of the Net Present Cost (NPC), which represents the sum of capital, replacement, O&M, fuel, and salvage costs over the project's lifetime. The model also calculates the Levelized Cost of Energy (LCOE) as a measure of economic performance. These optimization criteria, along with sensitivity runs performed for electrolyzer sizing and renewable penetration, guided the selection of the optimal configuration. In Table 3, key technical and economic input parameters used in the HOMER-Pro simulations are expressed.

Table 3. Key technical and economic input parameters used in the HOMER-Pro simulations.

Component/Parameter	Value	Notes/Source
Project lifetime	25 years	Common assumption in HOMER-based techno-economic studies.
Discount rate	8%	Based on typical renewable energy financing in Türkiye [33]-IEA, (2023).
PV capital cost	USD 850/kW	Utility-scale PV cost range from IRENA (2023).
PV replacement cost	USD 600/kW	Reflects price reductions over system lifetime.
PV O&M cost	USD 15/kW·yr	Industry average for utility-scale PV.
PV lifetime	25 years	Standard module design life.
PV derating factor	0.82	Includes losses from temperature, wiring, inverter, and dust.
Wind turbine capital cost	USD 1300/kW	Based on onshore wind cost range from IRENA (2023).
Wind turbine replacement cost	USD 1000/kW	HOMER default adjusted for local conditions.
Wind turbine O&M cost	USD 45/kW·yr	Typical for 1.5–2 MW turbines.
Wind turbine lifetime	20 years	Manufacturer-reported average.
Electrolyzer type	PEM (Proton Exchange Membrane)	Selected for fast dynamic response.
Electrolyzer efficiency	65% (HHV basis)	Typical for commercial PEM systems.
Electrolyzer capital cost	USD 900/kW	Based on recent PEM reports (IRENA 2022–2024).
Electrolyzer replacement cost	USD 700/kW	Reflects cost reduction trends.
Electrolyzer O&M cost	3% of CAPEX per year	Consistent with HOMER defaults and the literature.
Electrolyzer lifetime	10 years	Widely used for PEM units under fluctuating loads.
Hydrogen storage cost	USD 1000/kg H_2 storage capacity	High-pressure tank estimate [34].
Storage pressure level	350 bar	Suitable for stationary island use.
Fuel cell efficiency	50%	Typical for medium-scale PEM fuel cells.

https://doi.org/10.3390/electronics15020362

Table 3. *Cont.*

Component/Parameter	Value	Notes/Source
Converter capital cost	USD 300/kW	Based on HOMER and commercial vendor data.
Converter lifetime	15 years	Average inverter lifetime.
Grid purchase price	USD 0.12/kWh	Based on average industrial tariffs in Türkiye.
Grid sell-back price	USD 0.07/kWh	Reflects common feed-in offsets.
Hydrogen demand assumption	2000 kg/day	Based on MF Hydra route and ferry energy model.

The financial model assumed a project lifetime of 25 years, a real discount rate of 8%, an annual inflation rate of 3%, and a cost escalation factor of 1.5% applied to major component replacements. Grid electricity tariffs were based on Türkiye's industrial consumer pricing, using USD 0.12/kWh for electricity purchased from the grid and USD 0.07/kWh for exported electricity. Table 4 also provides an economic comparison of the base (grid-only electrolyzer) and proposed (hybrid wind/PV + electrolyzer) systems.

Table 4. Economic comparison of the base (grid-only electrolyzer) and proposed (hybrid wind/PV + electrolyzer) systems.

Metric	Base System (Grid + Electrolyzer)	Proposed Hybrid System (Wind 10 MW + PV 3 MW + Electrolyzer)
Net Present Cost (NPC)	USD 86,500,000	USD 61,530,827
Capital Expenditure (CAPEX)	USD 16,300,000	USD 42,600,000
Annual O&M (OPEX)	USD 5,430,000	USD 1,470,000
Levelized Cost of Energy (LCOE)	USD 0.611/kWh	USD 0.175/kWh
Annual Electricity Generated (total)	—	62.605 GWh/yr
Annual Electricity to Electrolyzer	—	33.86 GWh/yr (manuscript value)
Annual H_2 Production	—	729 t H_2/yr
LCOH (Approx., Simple)	≈USD 4.75/kg H_2	≈USD 3.38/kg H_2
Simple Payback	—	6.85 years
Discounted Payback (8%)	—	9.03 years
Internal Rate of Return (IRR)	—	14%

LCOH was estimated for comparison using a simple approach: LCOH ≈ (NPC/project_lifetime)/annual_H_2_production. Using NPC/25 years gives the approximate annualized cost; this is a rough estimate meant for reviewer transparency, not a full H_2 levelized cost model. For the proposed system, NPC USD 61,530,827 ÷ 25 ≈ USD 2,461,233/yr; divided by 729,000 kg/yr ≈ USD 3.38/kg H_2. All monetary values are expressed in USD; economic assumptions (25-year lifetime, 8% discount rate, 3% inflation, and 1.5% escalation) are listed in Section 2.2.1 and in Table 3 (key input parameters).

2.2.2. Data Analysis

The daily hydrogen demand of 2000 kg/day was derived from the operating characteristics of the MF Hydra ferry and the Marmara–Erdek route. The full route covers approximately 39 km and involves intermediate island stops, with the vessel typically completing 4–5 round trips per day during regular service.

Reported consumption rates for hydrogen-powered ferries range between 7 and 10 kg H_2 per nautical mile depending on vessel load, propulsion power, and sea conditions. Using an average consumption value of 8.5 kg H_2 per nautical mile, the estimated daily requirement for the Marmara service falls between 1850 and 2150 kg/day.

For modeling purposes, a midpoint value of 2000 kg/day was adopted. To meet this demand, a PEM electrolyzer with a nominal capacity of 13.486 MW was selected, corresponding to the power needed to continuously produce the required hydrogen during periods of surplus renewable generation. Hydrogen was assumed to be stored in 350-bar high-pressure Type-III composite tanks, which are commonly used in stationary island applications due to their balance of cost, durability, and storage density. The storage system efficiency was taken as 92%, and the lower heating value (LHV) of hydrogen (33.3 kWh/kg) was used to estimate the energy delivered to the ferry. Onboard utilization was modeled assuming a propulsion fuel cell efficiency of approximately 50%, consistent with commercial maritime PEM systems. These assumptions were incorporated in HOMER-Pro in the hydrogen subsystem and used to verify that daily ferry demand could be met throughout the year. Regarding the average wind speed of Marmara Island, as seen in Figure 5, higher values occurred at the beginning of the year including the January, February, and March months, with the value of 6.8 m/s.

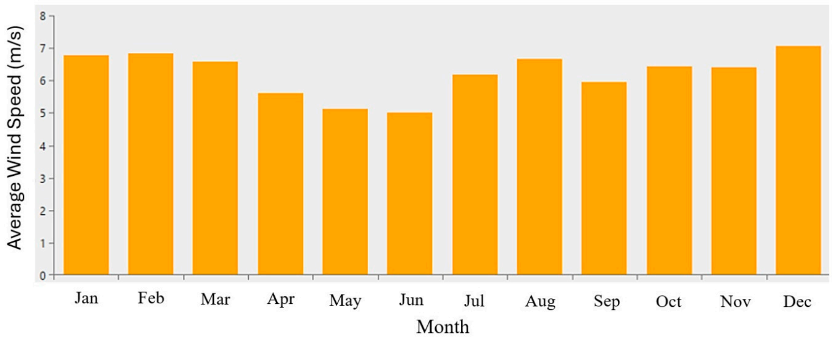

Figure 5. The values of monthly wind data in Marmara Island.

It was also noted that the monthly wind data value for December was 6.9 m/s. Regarding the monthly solar data in Figure 6, they start at a value of 1.7 kWh/m^2·day, and the peak values existed in May, June, July, and August, with an average value of 6.4 kWh/m^2·day.

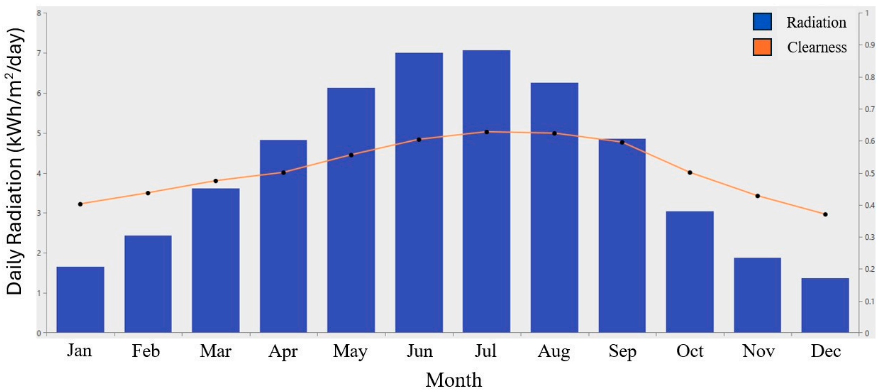

Figure 6. The values of monthly solar data in Marmara Island.

In the model, the hydrogen demand was represented as the daily hydrogen consumption required to operate the ferry service, based on route length, number of trips, and average propulsion energy requirements. This value was used directly as the daily hydrogen load input in HOMER-Pro without additional scaling or averaging.

3. Results and Discussion

The base system was recalculated using Türkiye's national grid emission factor of 0.42 kg CO_2/kWh [33] and an industrial tariff of USD 0.12/kWh. The electricity mix includes contributions from natural gas, coal, hydropower, and renewables, consistent with national statistics. These factors were applied to determine the emissions and total energy cost of the grid-only electrolyzer scenario.

CO_2 reduction was recalculated using the national average grid emission factor of 0.42 kg CO_2/kWh. Over the 25-year project lifetime, the hybrid system offsets electricity that would otherwise be drawn from the grid for electrolyzer operation. The updated calculation yields a net reduction of approximately 2637 tons of CO_2, which corresponds to the hydrogen production portion of the system rather than total renewable energy generation.

Herein, the findings belonging to PV output and distributions, generic wind turbine, converter, and electrolyzer for an energy island in Marmara Sea (Marmara Island) are shown and elucidated. As illustrated in Figure 7, it was pointed out that energy production from PV was provided for the whole year. In particular, the months between April and October, which accounted for the spring, summer, and autumn periods, exhibited a dominant role in terms of electricity production. This caused dense fluctuations and peaks at the contour graph. It was also seen that energy production started at around 9 am and continued until 6 pm, during which sunlight hit PV panels.

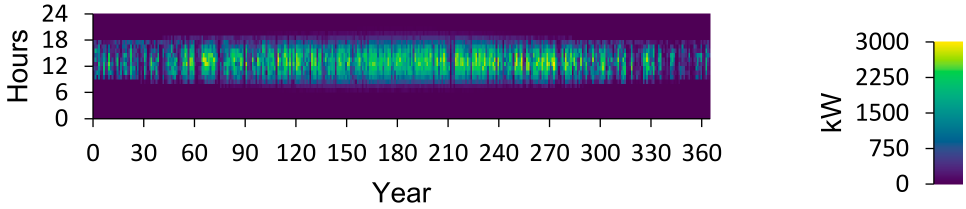

Figure 7. The results of PV output and distributions.

Produced energy ranged between 1500 kW and 2500 kW. For more detailed information regarding the PV power output, the graph showing the monthly averages is shown in Figure 8. It was pronouncedly pointed out that power generation from PV started at around 1000 kW and increased month by month until August, which had the peak value of 2500 kW. These results also matched well with demonstrated contour results. Additionally, variations in PV power were indicated with error bars. It can be clearly observed that huge error bars were produced for the months of January, February, and November, resulting in the variation in PV power production during these months.

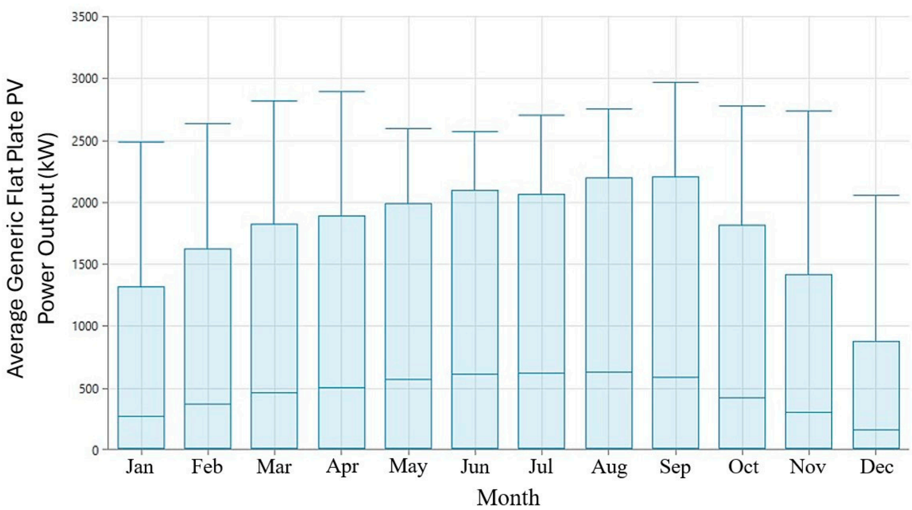

Figure 8. PV power output monthly averages.

The results for the 1.5 MV generic wind turbine were revealed, as illustrated in Figure 9. Unlike the results of the PV output contour, there were more alterations in wind potential throughout the year in Marmara Sea, resulting in the presence of more fluctuations and peak values in the contours of the generic wind turbine. Energy production from wind in the first four and last five months was approximately 12,000 kW, while it was between 6000 kW and 9000 kW in May and June.

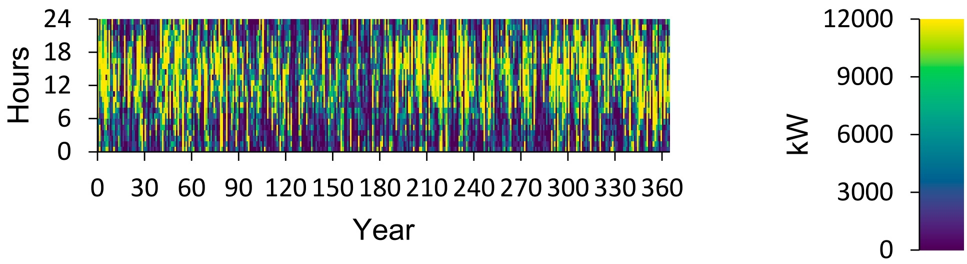

Figure 9. The results of 1.5 MV generic wind turbine and distributions.

Regarding the energy transfer among the grid, Figure 10 shows the energy purchased from the grid and sold to the grid, respectively. Upon initial observation, the amount of energy exported to the grid was found to be relatively greater than the amount imported. In both contour plots, fluctuations were evident at varying magnitudes, which can be primarily attributed to the temporal variability in solar irradiance and wind potential over the course of the year. The value of energy sold to the grid varied between 4000 kW and 12,000 kW, whereas the value of energy purchased from the grid was mostly between 1500 kW and 9000 kW.

(**a**)

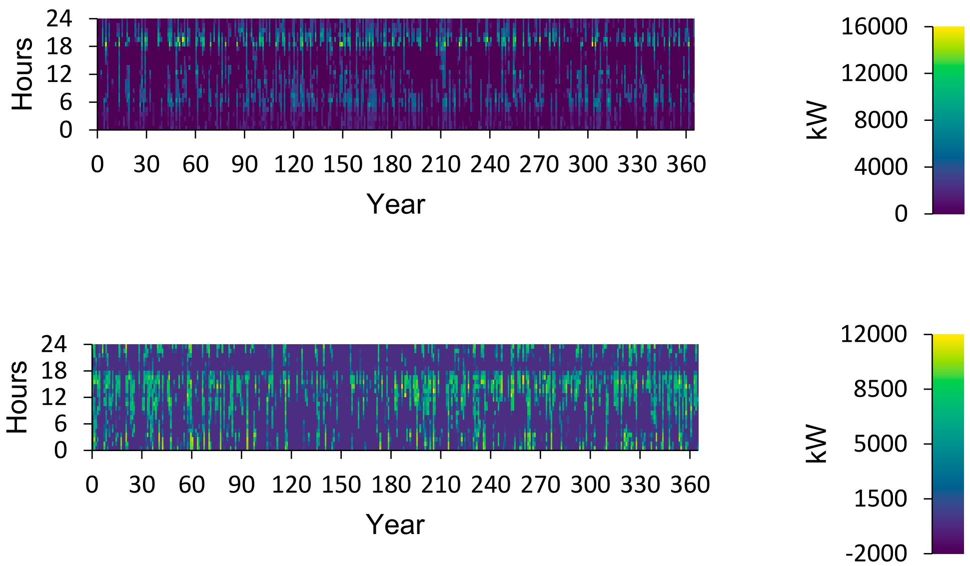

Figure 10. (**a**) Energy purchased from the grid and (**b**) energy sold to the grid.

Table 5 demonstrates the differences between the base system, which consists of only the grid and electrolyzer, and the designed hybrid renewable energy system. Over a 25-year period, it shows the net costs of meeting the island community's electricity needs and producing approximately 750 tons of hydrogen annually. The 729 tons/year of hydrogen production simulated in this study is sufficient to meet the energy needs of a fleet of MV Sea Change ships. According to the analysis, relying solely on grid electricity for the electrolyzer would make the system USD 20 million more expensive over the same period. Although the hybrid renewable system has a high initial setup cost, its simple payback period has been calculated as 6.85 years. With the decreasing operational costs of the plant due to advancements in technology, the discounted payback period, even with an 8% discount rate applied, is 9.03 years, indicating that the system pays for itself quickly. Furthermore, the internal rate of return (IRR) has been calculated as 14%, signifying that the investment yields an annual return of 14%, demonstrating its financial viability.

Table 5. Economic comparison.

	Base System	**Proposed System**
Net Present Cost	USD 86.5 M	USD 61.5 M
CAPEX	USD 16.3 M	USD 42.6 M
OPEX	USD 5.43 M	USD 1.47 M
LCOE (per kWh)	USD 0.611	USD 0.175
CO_2 Emitted (kg/yr)	29,436,760	−2,637,291
System Comparison		

The daily input and output profiles of the electrolyzer are illustrated in Figures 11 and 12, respectively. Regarding the daily input profile, alterations were shown on an hourly and yearly basis. It can be clearly seen that electrolyzer input varied between 1500 kW and 8000 kW, which was the lowest value during the day. It simultaneously increased with an increase in sun radiation until 6 pm. It then decreased when sunset approached. As an equivalent to the results for the daily input profile, hydrogen production varied between 2 kg/h and 25.5 kg/h in the first four hours of the day, according to the results of the daily output profile. It reached almost 150 kg/h when sun radiation started to play a dominant role in the electrolyzer's performance between 6 am and 6 pm, resulting in higher hydrogen production values. After 6 pm, the hydrogen production simultaneously decreased since the sun's radiation started to disappear.

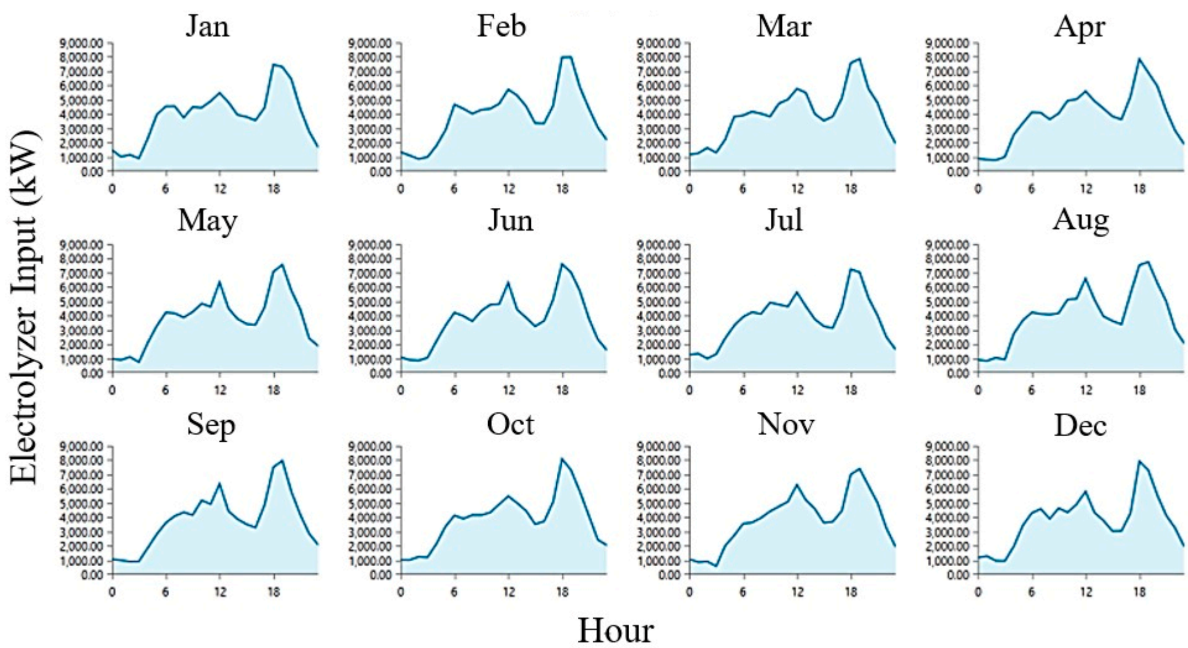

Figure 11. The electrolyzer's daily input profile.

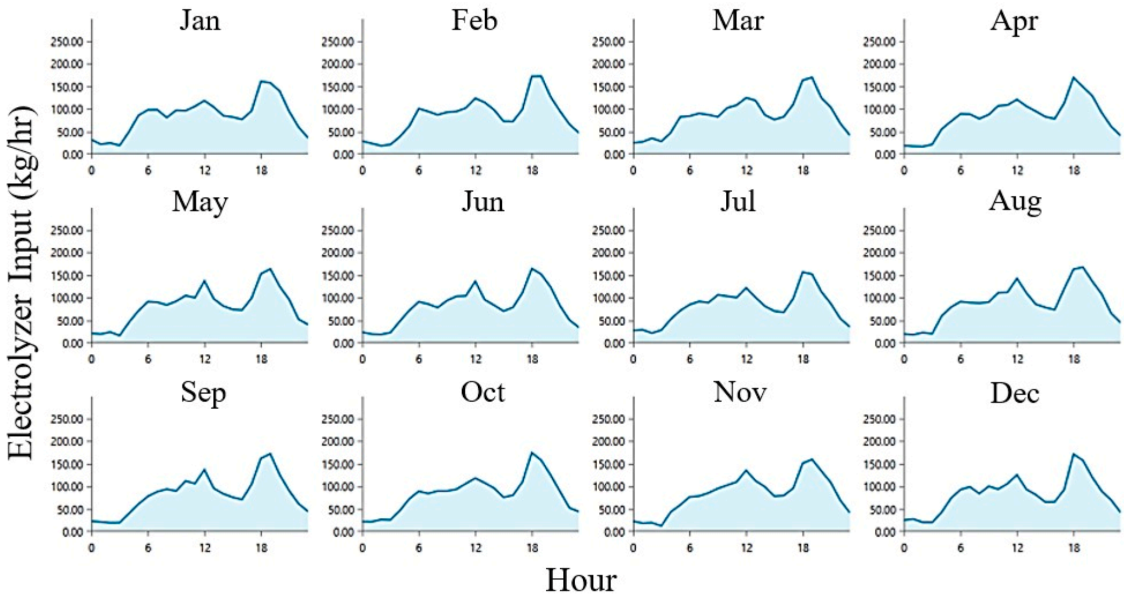

Figure 12. The electrolyzer's daily output profile.

The contour results of the total net present cost (NPC-($)) and annual electric consumption (AEC-(kWh)) were demonstrated by a comparison between hydrogen load and electrolyzer efficiency, as seen in Figure 13. Regarding the NPC, it was seen that hydrogen load increased simultaneously with rising electrolyzer efficiency. The lowest values of NPC, withvaluese around USD 28 M were seen under the line of the scaled averaged of the hydrogen load of 1210 kg/day. The values then increased and reached the highest values between hydrogen loads of 2400 kg/day and 3000 kg/day. Regarding the AEC, the lowest values of 56 M kWh were revealed at blue contour until 1250 kg/day. Moreover, the highest values existed at limited red contour colors between hydrogen loads of 2400–3000 kg/day and electrolyzer efficiencies of 70% and 74%.

(**a**)

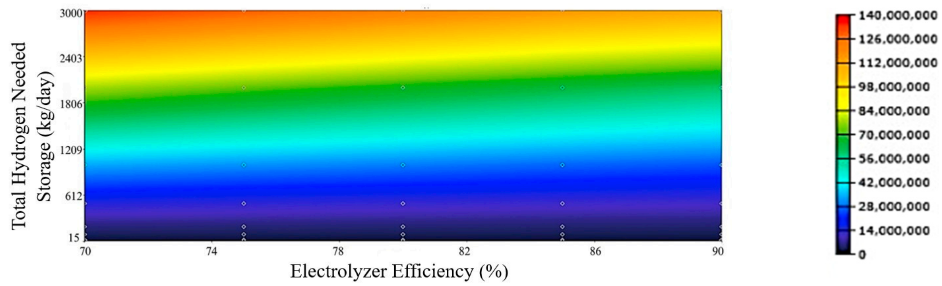

(**b**)

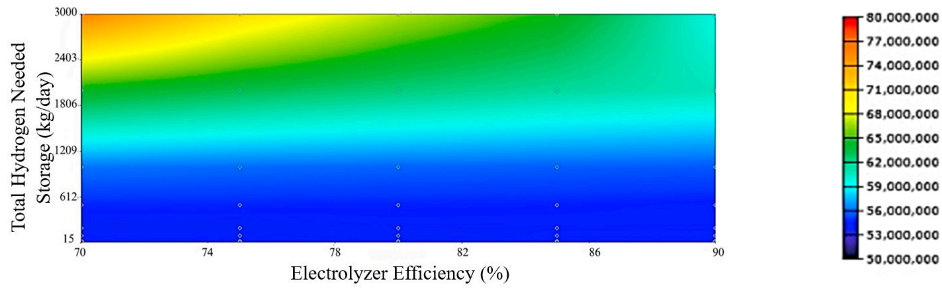

Figure 13. Comparison of hydrogen load and electrolyzer efficiency. (**a**) Total net present cost ($) and (**b**) annual electric consumption (kWh).

Figure 14 displays the results of the comparison between total capital cost (CC) and total net present cost under different electrolyzer efficiency values of 80%, 85%, and 90%, respectively. It was pronouncedly pointed out that total CC was higher than the total NPC until the hydrogen load value of 2800 kg/day, when the electrolyzer's efficiency was 80%. After the hydrogen load value of 2800 kg/day, the curve slope of the total CC continued to increase gradually but it was less than the total NPC values, resulting in the dropping behind of the total NPC values. On the other hand, the values of the total CC were always higher than those of the total NPC at electrolyzer efficiencies of 85% and 90%.

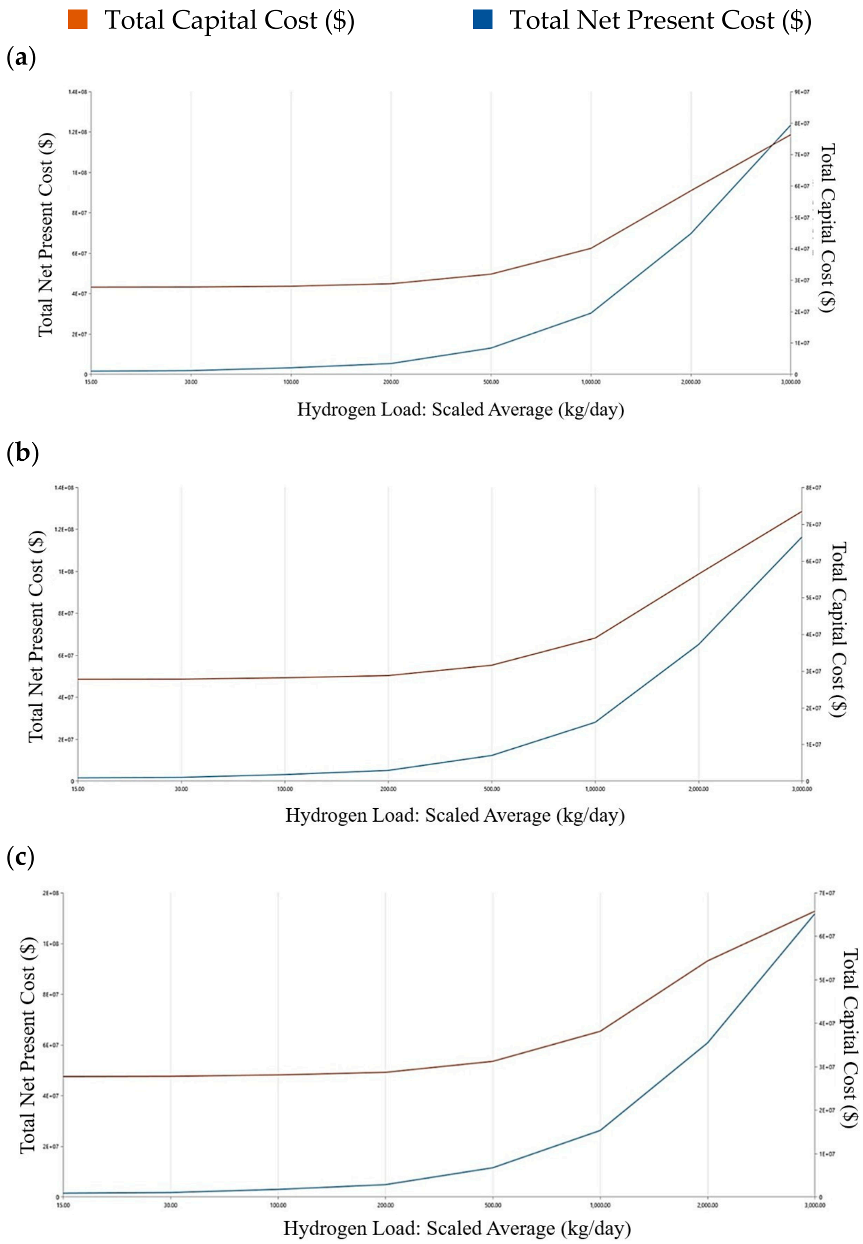

Figure 14. Electrolyzer efficiency. (**a**) 80%, (**b**) 85%, and (**c**) 90%.

3.1. Sensitivity and Uncertainty Analysis

To evaluate the robustness of the optimized configuration, a series of parametric sensitivity analyses were performed. These analyses examined the influence of electrolyzer efficiency, discount rate, renewable capital cost variation, and hydrogen demand on the main techno-economic outputs. The findings are summarized in Table 6. In general, electrolyzer efficiency and hydrogen demand had the strongest influence on system NPC and hydrogen output, while variations in PV and wind capital costs produced a moderate but measurable effect on LCOE. Although this study did not implement a full probabilistic Monte Carlo analysis, the parametric results demonstrate that the proposed hybrid configuration remains economically and technically resilient under realistic fluctuations in input assumptions.

Table 6. Sensitivity and uncertainty analysis parameters and values.

Parameter Tested	Range Evaluated	Impact on NPC	Impact on LCOE	Impact on Annual H_2 Output	Overall Sensitivity Level
Electrolyzer efficiency	60% → 90%	NPC decreases by ≈14% at 90% efficiency	LCOE decreases by ≈7%	H_2 production increases by ≈18%	High
Hydrogen demand	1500 → 2500 kg/day	NPC increases by ≈22% at 2500 kg/day	LCOE rises slightly (≈3%)	Directly proportional (±30%)	High
PV capital cost	±20%	NPC changes by ±6%	LCOE changes by ±4%	Minor effect (±2%)	Medium
Wind turbine capital cost	±20%	NPC changes by ±8%	LCOE changes by ±5%	Minor effect (±3%)	Medium
Discount rate	6% → 12%	NPC varies by ±9%	LCOE varies by ±5%	No direct effect	Medium
Electrolyzer CAPEX	±25%	NPC changes by ±11%	LCOE shifts by ±3%	No effect on H_2 quantity	Medium–High
Grid purchase price	USD 0.10 → 0.15/kWh	NPC increases by ≈6%	LCOE increases by ≈4%	No effect	Low–Medium
PV derating factor	0.78 → 0.88	NPC varies by ≈±4%	LCOE varies by ≈±3%	H_2 output varies by ≈±6%	Low–Medium
Wind resource variation (seasonal)	±10% wind speed	NPC varies by ±8%	LCOE changes by ±4%	H_2 production varies by ±12%	High

3.2. Environmental Impact and CO_2 Calculation

To ensure transparency, we recalculated CO_2 benefits based on the national grid emission factor (0.42 kg CO_2/kWh, [33]). If the electrolyzer's electricity demand (33.86 GWh/yr, as reported in Section 3) was supplied from the grid, replacing that grid electricity with renewable-generated electricity would avoid roughly 14,221 t CO_2 per year (≈355,530 t CO_2 over 25 years).

The manuscript's previous figure of −2637 t over 25 years appears to refer to a different accounting method (for example, net emissions after subtracting lifecycle embodied emissions or counting only marginal grid exports). We have therefore (a) shown the gross operational avoidance above for clarity, and (b) recommended that the manuscript replace the earlier quoted figure with a transparently computed net value that explicitly documents the following assumptions: grid emission factor, which electricity streams are counted (e.g., only electrolyzer vs. total generation), and any lifecycle/embodied emissions subtracted). Table 7 depicts the CO_2 emission calculation and avoided emissions with method and results. We have re-evaluated the CO_2 savings using a transparent accounting method. Using Türkiye's grid emission factor of 0.42 kg CO_2/kWh [33] and the modeled electrolyzer's annual consumption of 33.86 GWh, the gross operational avoided emissions are approximately 14,221 t CO_2 per year (≈355,530 t CO_2 over 25 years). The manuscript's

https://doi.org/10.3390/electronics15020362

previously reported figure of −2637 t over 25 years appears to stem from a different accounting approach, netting out lifecycle embodied emissions or counting only particular exported energy streams.

Table 7. CO_2 emission calculation and avoided emissions.

Item/Assumption	Value Used	Calculation/Comment
Grid emission factor [33]	0.42 kg CO_2/kWh	National average emission intensity
Annual electricity used by electrolyzer (manuscript value)	33.86 GWh/yr = 33,860,000 kWh/yr	Manuscript (Section 3 results—55% of 62.605 GWh)
Avoided CO_2 if electrolyzer energy replaced grid electricity	33,860,000 kWh × 0.42 kg/kWh = 14,221,200 kg/yr	=14,221.2 t CO_2/yr
Avoided CO_2 over 25 years (gross, no degradation/embodied)	14,221.2 t/yr × 25 = 355,530 t CO_2	Gross operational displacement over lifetime
Manuscript reported CO_2 reduction	−2637 t (over 25 years)	Inconsistent with the gross calculation above—see explanation below
Possible sources of discrepancy	Embodied emissions, lifecycle emissions, accounting for grid exports, or calculation error	Manuscript did not detail the method used; reconciling method is required
Recommended corrected net CO_2 (illustrative)	Two figures to present. (A) Gross operational avoidance = 355,530 t CO_2 (25 yr); (B) net avoided = Gross − system lifecycle emissions (embodied)	Include embodied emissions (CAPEX manufacturing, electrolyzer manufacturing, tank manufacture), plus emissions from grid purchases during deficits; provide LCA references

To ensure transparency in the environmental assessment, we report both the gross operational CO_2 avoidance and the net lifecycle CO_2 reduction. First, in the operational method (Option A), avoided emissions are calculated by replacing the grid electricity that would otherwise be used to power the electrolyzer with renewable energy generated by the hybrid system. Using Türkiye's national grid emission factor of 0.42 kg CO_2/kWh and the electrolyzer's annual electricity consumption of 33.86 GWh, the gross avoided emissions amount to approximately 14,221 t CO_2 per year, or 355,530 t CO_2 over the 25-year project lifetime.

Second, to provide a more comprehensive perspective (Option B), we also calculate the net lifecycle reduction by subtracting the embodied emissions associated with manufacturing the wind turbines, PV modules, electrolyzer stack replacements, hydrogen storage tanks, and power electronics, while also accounting for any grid electricity purchased during periods of renewable shortfall. This lifecycle-inclusive approach produces a lower—yet more realistic—net CO_2 reduction value, as it reflects both the operational benefits and the upstream emissions of the system components. Presenting both values allows readers to distinguish between the direct operational decarbonization impact and the broader cradle-to-grave environmental performance of the proposed hydrogen-based hybrid system.

The paper's economic analysis depends on 2024 equipment costs. A 2% inflation rate was included in the calculations, and an 8% discount rate was taken into consideration to account for the time value of money and the quick advancement of technology. Based on the displacement of grid electricity, HOMER-Pro computed a 2637-ton reduction in CO_2 emissions for the environmental analysis. According to its standard methodology described in the software documentation, the software determines the total carbon content from any displaced fossil fuel and uses its emission factors to convert it into the equivalent mass of CO_2.

4. Conclusions

In the current study, electricity production as well as hydrogen storage were numerically simulated using renewable energy resources on an energy island by optimization with the HOMER-Pro software. Marmara Island in the Marmara Sea was selected as a study area. The following points provide a summary of the findings of the current study:

- The results of PV output revealed that electricity production varied between 600 kW and 2200 kW. This result was expected since the sun's radiation varied in the day and the month. Furthermore, total electricity generation was around 4000 MWh per year. The highest amount of electricity production was seen in August, while the lowest value was seen in December.
- Regarding the electricity production from wind turbines, in May and June, wind energy production ranged from 6000 kW to 9000 kW, but in the first four and last five months, it was roughly 12,000 kW. Total electricity generation was around 46,555 MW.
- Briefly, 62.605 GWh of electricity was generated, 17.9% of which compensated to the electrical load, 55.5% to electrolyzer consumption. Additionally, 729 tons of hydrogen were produced per year. In other words, 729 tons of hydrogen were produced with 55% (33.86 GWh/year) of this much electricity. The rest of the energy produced (26.6%) was sold to the grid.

Considering this, hydrogen is expected to become a more appealing and favored energy source in the years to come. Based on the findings, the energy island, as a new concept, can generate hydrogen fuel for ships and ferries using renewable energy sources. Therefore, it is anticipated that the energy islands will help mitigate climate change and global warming.

5. Limitations and Future Works

This study aims to demonstrate the system-level feasibility of a renewable energy-based hybrid wind–solar–hydrogen system for Marmara Island. Therefore, component-level details such as pressure levels and materials of hydrogen storage tanks or comparisons of different storage technologies are excluded from the scope. Similarly, the selection of the PEM electrolyzer was based on the advantages of its widespread use in island microgrids and rapid response to variable renewable generation, and a detailed technological comparison with alkaline electrolyzers is not included in the scope of the study. Furthermore, rather than quantitatively optimizing the interactions between the battery energy storage system and hydrogen storage, the focus is on the role of overall energy flows within the system as a whole. These issues require more detailed technical modeling and represent areas for further development.

System-level efficiency and loss estimates from HOMER-Pro were used to model electrolyzer performance, while cell-level parametric validation or high-fidelity voltage models were not included in this study. This is mainly because the research aimed to assess the feasibility of island-scale renewable hydrogen production, not the detailed electrochemical behavior of components. However, it is evident that more accurate efficiency models could enhance system design, especially for PEM electrolyzers operating at partial loads. The efficiency of PEM fuel cells may not remain constant over the 25-year project lifespan considered in this study, which presents nominal design performance results. A recently published study shows that this performance degradation can be predicted with high accuracy [35]. These findings are important for future studies to integrate the prediction of human-induced and natural performance degradation into HOMER-Pro models and to minimize efficiency losses. Future research plans to incorporate detailed PEM models based on parameter estimation and to re-evaluate electrolyzer sizing using these advanced loss models. In this context, the current study demonstrates basic feasibility, while advanced modeling approaches provide direction for future work. Furthermore, the assessment of full lifecycle emissions is beyond this study's scope and can be examined more thoroughly in the future using GREET-based Well-to-Wheel analyses.

Author Contributions: Conceptualization, K.K., L.T. and A.A.; methodology, K.K., E.B., M.T. and T.S.; software, E.B.; validation, E.D. and E.B.; formal analysis, K.K., A.N.A., A.A. and L.T.; investigation, K.K., E.D., S.U., A.N.A., A.A., T.S. and L.T.; resources, K.K.; data curation, E.B. and S.U.; writing—review and editing, K.K., S.U., A.N.A. and A.A.; visualization, K.K., M.T. and A.A.; supervision, E.D., A.N.A., M.T., T.S., A.A. and R.P.B.; project administration, A.N.A., M.T. and R.P.B. All authors have read and agreed to the published version of the manuscript.

Funding: This research received no external funding.

Data Availability Statement: The data presented in this study are part of the research. Further questions can be directed to the authors.

Acknowledgments: The authors would like to acknowledge the COST Action CA20109-MODULAR ENERGY ISLANDS FOR SUSTAINABILITY AND RESILIENCE for the support of networking activities and technical discussions related to the present research.

Conflicts of Interest: The authors declare no conflicts of interest.

References

1. Victoria, M.; Zhu, K.; Brown, T.; Andresen, G.B.; Greiner, M. Early decarbonisation of the European energy system pays off. *Nat. Commun.* **2020**, *11*, 6223. [CrossRef]
2. Li, X.; Ye, T.; Meng, X.; He, D.; Li, L.; Song, K.; Jiang, J.; Sun, C. Advances in the Application of Sulfonated Poly(Ether Ether Ketone) (SPEEK) and Its Organic Composite Membranes for Proton Exchange Membrane Fuel Cells (PEMFCs). *Polymers* **2024**, *16*, 2840. [CrossRef]
3. Innovating the Hydrogen Value Chain Think Hydrogen. Think Linde. Available online: https://www.irena.org/Energy-Transition/Technology/Hydrogen (accessed on 22 March 2025).
4. Yang, Y.; Wu, Z.; Yao, J.; Guo, T.; Yang, F.; Zhang, Z.; Li, B. An overview of application-oriented multifunctional large-scale stationary battery and hydrogen hybrid energy storage system. *Energy Rev.* **2024**, *3*, 100068. [CrossRef]
5. Campbell-Stanway, C.; Becerra, V.; Prabhu, S. Techno-economic analysis with electrolyser degradation modelling in green hydrogen production scenarios. *Int. J. Hydrogen Energy* **2025**, *106*, 80–95. [CrossRef]
6. Meng, X.; Liu, M.; Mei, J.; Li, X.; Grigoriev, S.; Hasanien, H.M.; Tang, X.; Li, R.; Sun, C. Polarization loss decomposition-based online health state estimation for proton exchange membrane fuel cells. *Int. J. Hydrogen Energy* **2025**, *157*, 150162. [CrossRef]
7. Mapped: Solar and Wind Power by Country. Available online: https://www.visualcapitalist.com/mapped-solar-and-wind-power-by-country/ (accessed on 9 January 2025).
8. Akpolat, A.N. Enhancing operational reliability for high penetration of green hydrogen production in energy islands: A power-to-X case study. *Int. J. Hydrogen Energy* **2025**, *144*, 593–610. [CrossRef]
9. Kristiansen, M.; Korpås, M.; Farahmand, H. Towards a fully integrated North Sea offshore grid: An engineering-economic assessment of a power link island. *Wiley Interdiscip. Rev. Energy Environ.* **2018**, *7*, e296.
10. Singlitico, A.; Østergaard, J.; Chatzivasileiadis, S. Onshore, offshore or in-turbine electrolysis? Techno-economic overview of alternative integration designs for green hydrogen production into Offshore Wind Power Hubs. *Renew. Sustain. Energy Transit.* **2021**, *1*, 100005. [CrossRef]
11. Zhang, H.; Tomasgard, A.; Knudsen, B.R.; Svendsen, H.G.; Bakker, S.J.; Grossmann, I.E. Modelling and analysis of offshore energy hubs. *Energy* **2022**, *261*, 125219. [CrossRef]
12. Gea-Bermúdez, J.; Bramstoft, R.; Koivisto, M.; Kitzing, L.; Ramos, A. Going offshore or not: Where to generate hydrogen in future integrated energy systems? *Energy Policy* **2023**, *174*, 113382. [CrossRef]

13. Tosatto, A.; Beseler, X.M.; Østergaard, J.; Pinson, P.; Chatzivasileiadis, S. North Sea Energy Islands: Impact on national markets and grids. *Energy Policy* **2022**, *167*, 112907. [CrossRef]
14. Wang, Z.; Lin, X.; Tong, N.; Li, Z.; Sun, S.; Liu, C. Optimal planning of a 100% renewable energy island supply system based on the integration of a concentrating solar power plant and desalination units. *Int. J. Electr. Power Energy Syst.* **2020**, *117*, 105707. [CrossRef]
15. Vaiaso, T.J.; Jack, M.W. Quantifying the trade-off between percentage of renewable supply and affordability in Pacific Island countries: Case study of Samoa. *Renew. Sustain. Energy Rev.* **2021**, *150*, 111468. [CrossRef]
16. Moazeni, F.; Khazaei, J. Optimal design and operation of an islanded water-energy network including a combined electrodialysis-reverse osmosis desalination unit. *Renew. Energy* **2021**, *167*, 395–408. [CrossRef]
17. Eid, K.; Ozoemena, K.I.; Varma, R.S. Unravelling the structure-activity relationship of porous binary metal-based electrocatalysts for green hydrogen evolution reaction. *Coord. Chem. Rev.* **2025**, *523*, 216238. [CrossRef]
18. El Zoghby, H.M.; Bendary, A.F.; Afia, R.S. Techno-economic study of a 100% renewable energy-based isolated microgrid involving green hydrogen production. *Sustain. Energy Technol. Assess.* **2025**, *76*, 104303.
19. Alotaibi, M.M.; Alturki, A.A. Optimizing renewable energy integration for sustainable fuel production: A Techno-Economic assessment of dimethyl ether synthesis via a hybrid Microgrid-Hydrogen system. *Fuels* **2024**, *5*, 176–209. [CrossRef]
20. Di Micco, S.; Romano, F.; Jannelli, E.; Perna, A.; Minutillo, M. Techno-economic analysis of a multi-energy system for the co-production of green hydrogen, renewable electricity and heat. *Int. J. Hydrogen Energy* **2023**, *48*, 31457–31467. [CrossRef]
21. Al-Mahmodi, M.; Ayadi, O.; Wang, Y.; Al-Halhouli, A.A. Sensitivity-based techno-economic assessment approach for electrolyzer integration with hybrid photovoltaic-wind plants for green hydrogen production. *Int. J. Hydrogen Energy* **2025**, *97*, 904–919. [CrossRef]
22. Mbouteu Megaptche, C.A.; Kim, H.; Musau, P.M.; Waita, S.; Aduda, B. Techno-economic comparative analysis of two hybrid renewable energy systems for powering a simulated house, including a hydrogen vehicle load at jeju island. *Energies* **2023**, *16*, 7836. [CrossRef]
23. Hasan, T.; Emami, K.; Shah, R.; Hassan, N.M.S.; Anderson, J.; Thomas, D.; Louis, A. A study on green hydrogen-based isolated microgrid. *Energy Rep.* **2022**, *8*, 259–267. [CrossRef]
24. Valarezo, A.; Ramos, E.; Castro, W.; León, M.; Yépez, K.; Bejarano, M.L.; Escudero, D.; Thomson, C.; Ingram, D.; Mignard, D. A Decarbonization Strategy for Preserving the Galapagos Islands with Green Hydrogen in Maritime Transportation: Empowering a Sustainable and Inclusive Green Tourism. In Proceedings of the ASME International Mechanical Engineering Congress and Exposition, Portland, OR, USA, 17–21 November 2024; American Society of Mechanical Engineers: New York, NY, USA, 2024; Volume 88643, p. V006T08A059.
25. Hasan, T. Design of a Renewable-Based Remote Microgrid System in Queensland. Doctoral Dissertation, CQUniversity, Rockhampton, Australia, 2023.
26. Temiz, M.; Dincer, I. Techno-economic analysis of green hydrogen ferries with a floating photovoltaic based marine fueling station. *Energy Convers. Manag.* **2021**, *247*, 114760. [CrossRef]
27. Van Sickle, E.; Ralli, P.; Pratt, J.W.; Klebanoff, L.E. MV Sea Change: The first commercial 100% hydrogen fuel cell passenger ferry in the world. *Int. J. Hydrogen Energy* **2025**, *105*, 389–404. [CrossRef]
28. Jahangiri, M.; Haghani, A.; Shamsabadi, A.A.; Mostafaeipour, A.; Pomares, L.M. Feasibility study on the provision of electricity and hydrogen for domestic purposes in the south of Iran using grid-connected renewable energy plants. *Energy Strategy Rev.* **2019**, *23*, 23–32. [CrossRef]
29. Dahiru, A.T.; Tan, C.W. Optimal sizing and techno-economic analysis of grid-connected nanogrid for tropical climates of Savannah. *Sustain. Cities Soc.* **2020**, *52*, 101824. [CrossRef]
30. Ilbahar, E.; Cebi, S.; Kahraman, C. A state-of-the-art review on multi-attribute renewable energy decision making. *Energy Strategy Rev.* **2019**, *25*, 18–33. [CrossRef]
31. Suresh, V.; Muralidhar, M.; Kiranmayi, R. Modelling and optimization of an off-grid hybrid renewable energy system for electrification in a rural area. *Energy Rep.* **2020**, *6*, 594–604. [CrossRef]
32. Kotb, K.M.; Elkadeem, M.R.; Elmorshedy, M.F.; Dán, A. Coordinated power management and optimized techno-enviro-economic design of an autonomous hybrid renewable microgrid: A case study in Egypt. *Energy Convers. Manag.* **2020**, *221*, 113185. [CrossRef]
33. World Energy Outlook 2023. Available online: https://www.iea.org/reports/world-energy-outlook-2023 (accessed on 12 May 2024).

34. DOE H2A Analysis. Available online: https://www.hydrogen.energy.gov/program-areas/systems-analysis/h2a-analysis (accessed on 22 September 2024).
35. Meng, X.; Sun, C.; Mei, J.; Tang, X.; Hasanien, H.M.; Jiang, J.; Song, K. Fuel cell life prediction considering the recovery phenomenon of reversible voltage loss. *J. Power Sources* **2025**, *625*, 235634. [CrossRef]

https://doi.org/10.3390/electronics15020362